Open Access

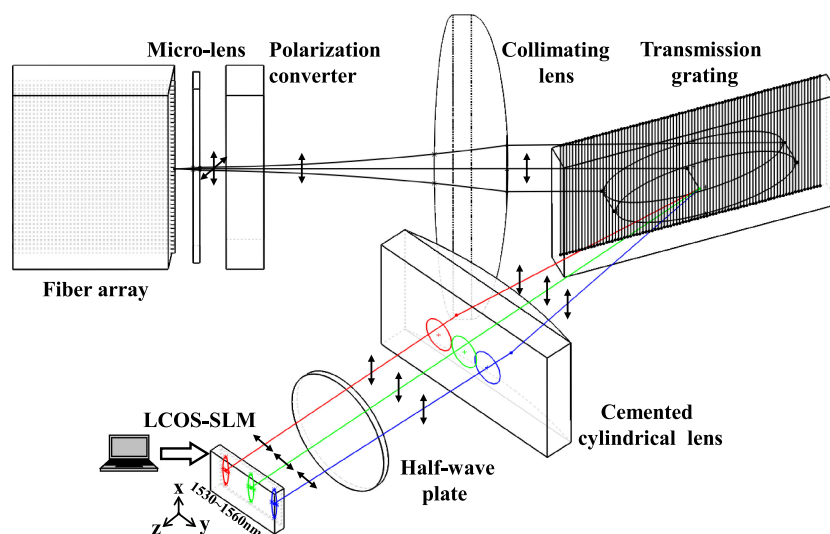# High-Resolution Tunable Filter With Flexible Bandwidth and Power Attenuation Based on an LCoS Processor

Yunshu Gao
Genxiang Chen
Xiao Chen
Qian Zhang
Qiao Chen
Ce Zhang
Kai Tian
Zhongwei Tan
Chao Yu

IEEE

High-Resolution Tunable Filter With Flexible Bandwidth and Power Attenuation Based on an LCoS Processor

Yunshu Gao [iD],[1,2] **Genxiang Chen,**[1] **Xiao Chen,**[1] **Qian Zhang,**[1] **Qiao Chen,**[1] **Ce Zhang,**[1] **Kai Tian,**[2] **Zhongwei Tan,**[2] **and Chao Yu**[3]

[1]College of Science, Minzu University of China, Beijing 100081, China
[2]School of Electronic and Information Engineering, Beijing Jiaotong University, Beijing 100044, China
[3]School of Electronic Engineering, Beijing University of Posts and Telecommunications, Beijing 100876, China

Abstract: High-resolution optical filters and wavelength selective switches are the essential components in the current and next-generation dynamic optical networks. A high-resolution programmable filter for telecom application is proposed and experimentally demonstrated based on a 4 k phase-only liquid crystal on silicon (LCoS) spatial light modulator. The tuning resolution, bandwidth, and power attenuation for each wavelength channel can be modulated independently by remote software control. For each channel, the center wavelength is tuned in the step of 7.5 $\pm$ 1 pm and the 3 dB bandwidth achieves from 10 GHz to 3 THz. Furthermore, by multi-casting hologram design techniques for an LCoS, the power attenuation is adjusted from 0 dB to 30 dB with the step of 0.1 dB. The insertion loss is less than 6 dB across the entire *C*-band and 1.8 dB of it can be further improved by adopting an LCoS chip with smaller reflection loss.

Index Terms: Optical filter, tunable filter, liquid crystal on silicon (LCoS), flexible bandwidth selection.

1. Introduction

To improve the flexibility and efficiency of current and next-generation wavelength division multiplexing (WDM) networks, the most promising solutions is to introduce elastic optical networks (EONs) that can dynamically allocate a flexible amount of spectral resources for individual channels to support different symbol rates. On the other hand, the high-order quadrature amplitude modulation (QAM) format with orthogonal frequency division multiplexing (OFDM) technology is expected to play the dominating role in future optical networking. Therefore, it requires the reconfigurable optical add/drop multiplexer (ROADM) nodes to support arbitrary flexible grid, variable symbol rates and modulation formats, which not only meet the 12.5 GHz frequency slot width of ITU-T G.694.1

standard, but also provide 10 GHz bandwidth and sub-GHz fine wavelength tuning to match OFDM signals [1]–[4]. In order to realize such functions, ROADMs must consist of high-resolution optical filters and channel switching devices, such as wavelength selective switches (WSS), wavelength blockers (WB) and tunable filters.

Nowadays,optical processors based on liquid crystal on silicon (LCoS) device combining with gratings have become an attractive solution for modulating spectrum resources [5]–[9]. An LCoS spatial light modulator is an array of electro-optic cells independently addressed by a Very-Large-Scale-Integrated circuit to generate a reconfigurable, reflective digital holographic diffraction grating capable of steering an optical beam along arbitrary directions. Up to date, most of LCoS devices applied in WSS have a pixel size larger than 6 μm, which limits the minimum spectral tuning resolution [10], [11]. Xie D [11] reported a 1 × 9 LCoS-based WSS with 8 μm pixel size and the tuning resolution is 6.25 GHz. In addition, some components like plano-convex cylindrical lenses used in the system are unable to focus the beam close to the diffraction limit due to the aberration, worsening the minimum spectral passband [10]. So the pixel size of LCoS and focusing ability of cylindrical lenses greatly influence the performance of tuning precision and bandwidth. On the other hand, how to increase the output ports is also important for information capacity in networks. To reduce the port space of fiber-coupling micro-lens array is an effective way. For example, Sakurai Y reported a 250 μm pitch micro-lens array into the wavelength blocker [12]. Iwama M applied a spot size converter (SSC) array with 127 μm spacing based on planar lightwave circuit (PLC) technology into the WSS [5], [7], however a micro-lens array with 127 μm pitch up to now has not been reported yet.

In this paper, we employ a fiber-coupling micro-lens array with 127 μm pitch and a GAEA LCoS device with the pixel pitch 3.74 μm produced by HOLOEYE Company into the optical system and experimentally demonstrate a high-resolution tunable filter with sub-GHz fine tuning, flexible bandwidth and power attenuation. Although the smaller pixel size leads to some negative physical effects, such as higher insertion loss (IL) and lower diffraction efficiency due to the lower filling factor, the benefits of improved resolution, narrow bandwidth and the larger diffraction angles have also made the latest-generation LCoS widely appealing as the core component in spectrum filtering and switching systems in future. Up to now, 1 × 9 WSS modules have been commercially deployed in optical networks by Cambridge University [13], the larger diffraction angle of LCoS and smaller pitch micro-lens array are expected to contribute for the higher port counts of WSS, which is greatly demanded for the next-generation smart optical networks. So the LCoS with a pixel pitch of 3.74 μm and micro-lens array with a spacing of 127 μm in this work are significant to the development of multi-ports WSS.

2. Optical Design of the Filter

The schematic of an assembled optical filter based on 2-f configuration is shown in Fig. 1, including a fiber-coupling micro-lens array, a polarization converter, a half-wave plate, two lenses, a transmission grating and an LCoS-SLM. The fiber-coupling micro-lens array comprises hundreds of fiber ports with $\delta = 127$ μm pitch. The micro-lens array needs to be accurately aligned with the fiber array in the system so as to minimize the alignment error of offset and tilt. The micro-lens array decreases the half-angle of beam divergence from 8° to 0.86°. The micro-lens array and collimating lens convert the input fiber Gaussian beam waist from 5.2 μm to 4.5 mm for matching with the width of an LCoS chip and covering enough pixels to achieve high diffraction efficiency.

We pick a fiber port as an input/output port to demonstrate the spectral resolving capability of the filter system. For the LCoS is P-polarization sensitive and the transmission grating is S-polarization dependent, a polarization converter is inserted to adjust the input polarization states and a polymer zero-order half-wave plate placed in front of the LCoS-SLM provides stable phase retardance over C-band in a wide incident angle.

The 1201.2 line/mm transmission grating is arranged at the focal plane of the cylindrical lens ($f_2 = 145$ mm) and the collimating lens ($f_1 = 300$ mm). When the near-parallel beam travels through the transmission grating, the optical signals from 1530 nm–1560 nm are angularly dispersed in
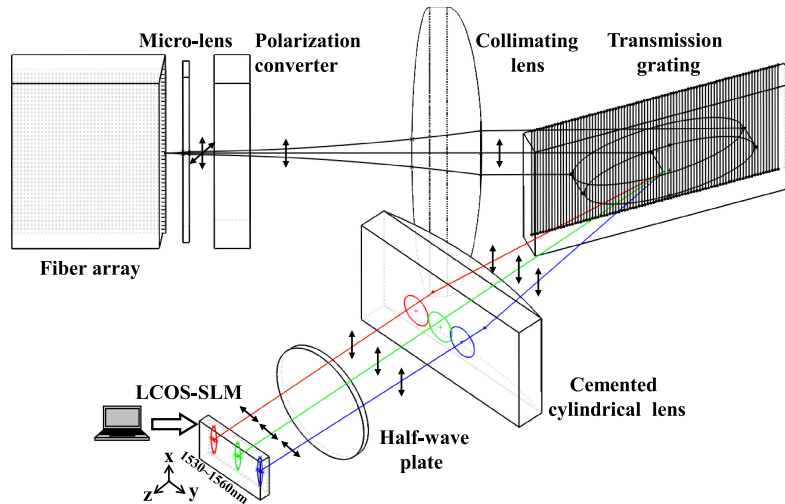
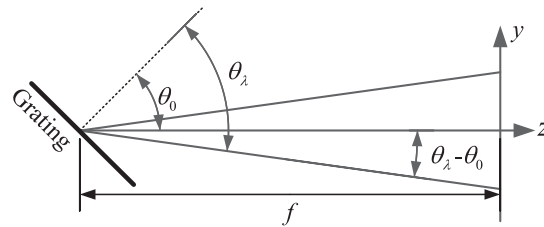Fig. 1. Schematic of tunable filter based on LCoS-SLM.

Fig. 2. Configuration of beam path after the grating diffraction.

y-axis direction and mapped on the different position of the LCoS chip which is placed at the same back focal plane of the collimating lens and cylindrical lens. The used LCoS-SLM consists of an array of 4094 × 2464 pixels (4 k × 2 k) on a pitch of 3.74 μm. By uploading optimized phase-only holograms on chip, we can select and steer arbitrary wavebands from the input fiber port to output ports.

The minimum spectral bandwidth is determined by the beam spot in y-axis on chip which is compressed by the cylindrical lens. As shown in Fig. 1, the cylindrical lens simultaneously demonstrates two functions: (1) focusing wavelength channels in y-axis direction; (2) collimating different wavebands. Note that the cemented cylindrical lens is adopted in the system to eliminate the aberration of optical components to improve the minimum passband.

The minimum spectral bandwidth B_{min} and tuning resolution R of center wavelength are two key specifications of filters. When wavebands are dispersed by a grating, the tilted grating causes inhomogeneous spectrum in space, leading to non-uniform distribution on an LCoS. It means B_{min} and R are both wavelength-dependent. As shown in Fig. 2, z-axis is configured along the optical path of 1545 nm, the middle wavelength in C-band. The position distribution $y(\lambda)$ is written as:

$$y(\lambda) = f \tan(\theta_\lambda - \theta_0) \tag{1}$$

The first-order diffraction angle θ_λ is determined by the grating equation:

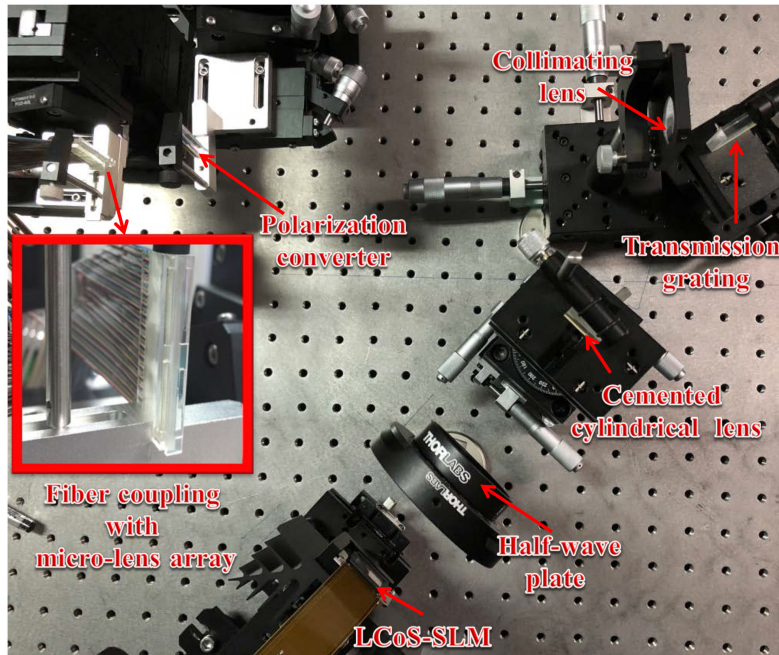$$d(\sin\theta_\lambda + \sin\theta_{in}) = \lambda \tag{2}$$

Fig. 3. System setup of the tunable optical filter.

where d is the groove width of grating, θ_{in} is the incident angle of 1545 nm and θ_{λ} is the corresponding diffraction angle. The derivative of y is

$$\frac{\partial y}{\partial \lambda} = \frac{f}{d \cos^2 (\theta_{\lambda} - \theta_0) \sqrt{1 - (\lambda/d - \sin \theta_{in})^2}} \tag{3}$$

Based on above equations, the tuning resolution R can be written as:

$$R = a \frac{\partial \lambda}{\partial y} = \frac{a d \cos^2 (\theta_{\lambda} - \theta_0) \sqrt{1 - (\lambda/d - \sin \theta_{in})^2}}{f} \tag{4}$$

where a is one pixel size on the LCoS and f is the focal length of a cylindrical lens. If the dispersed spectrum covers the whole working length of a LCoS, it is clear that the smaller pixel size a contributes for the finer tuning precision R according to Eq. (4).

The minimum spectral bandwidth B_{min} is shown as:

$$B_{min} = \frac{L}{a} R \tag{5}$$

where L the size of elliptical beam spot in y-axis on the LCoS. The minimum spot size in y-axis is proportional to the minimum spectral bandwidth.

The theoretical spot size can be estimated by the diffraction-limit formula:

$$L_{min} = \frac{4\lambda M^2 f}{\pi D} \tag{6}$$

where D is the beam diameter on the cylindrical lens, and M^2 is the beam quality parameter.

As the dispersed spectrum covers the length of an LCoS, B_{min} is only determined by the focusing ability of a cylindrical lens. It means that the elliptical spots on the LCoS needs to be elongated enough to obtain smaller passband. According to Eq. (3), the cylindrical lens with short focal length is helpful to decrease L_{min}, but the grooves density of a grating should increase to keep a wide dispersed spectrum in space.
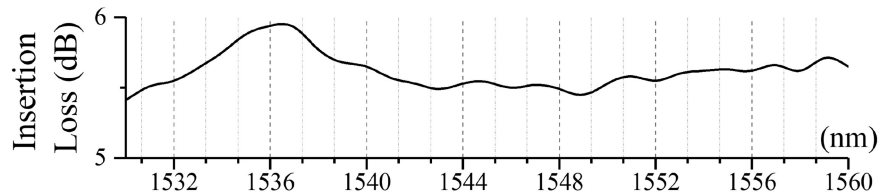
Fig. 4. Dependence of total insertion loss on C-band wavelength in filter.

3. Experiments and Discussions

The experimental arrangement of the optical filter is displayed in Fig. 3. To demonstrate the ability of sub-GHz fine tuning, free spectral bandwidth and flexible power attenuation, the amplified spontaneous emission (ASE) light source in 1530 nm–1560 nm is launched into the system as input signals. A YOKOGAWA: AQ6370C optical spectrum measurement analyzer with the resolution of 20 pm is applied to detect the performance.

Fig. 4 illustrates the fluctuation of total insertion loss is between 5.4 dB to 6.0 dB across the entire C-band. The IL is mainly caused by two aspects: the static and dynamic loss. The static loss includes 1.5 dB from the fiber-coupling micro-lens array, 0.5 dB from the polarization converter, 0.1 dB from the cylindrical lens, 0.1 dB from the collimating lens, 1.2 dB from the transmission grating, 0.1 dB from the half-wave plate and 1.8 dB diffraction loss from the 4k-LCoS. The dynamic loss is caused by asymmetric optical path of different wavelength passing through the slanted transmission grating, leading to 0.5 dB fluctuation loss. Measured intrinsic PDL within the passband of 12.5 GHz for the optical system is less than 0.8 dB.

The measured fiber-coupling efficiency of the micro-lens array is 70%, which is mainly caused by Fresnel reflection from the fiber end surface and axial misalignment of the micro-lens. Besides, the LCoS-SLM makes 1.8 dB loss by the reflection and diffraction. The reflection loss is 1.42 dB for this device. When a beam modulated by LCoS passes back through the polarization-sensitive grating, the effect of fringing electric field not only decreases the reflection efficiency, but also brings 0.8 dB IL for the incident linear-polarized light to the elliptical polarized light [14]. The small period blazed grating hologram on chip results in large diffraction angle and low diffraction efficiency due to the fringing electric field [14]. We therefore upload a large period hologram to minimize the diffraction loss to 0.3 dB. The other measured IL, such as the lens and half-wave plate, is caused by the aberration of optical components and different optical path of multi-wavelength.

In Fig. 5, by driving the LCoS with appropriate steering phase holograms, the center wavelength of the waveband with 3dB-bandwidth of 10 GHz can be tuned flexibly in the step of 7 pm (0.9 GHz) over the whole C-band. Furthermore, the bandwidth can also be digitally modulated with the resolution 0.69 GHz as shown in Fig. 6. So, arbitrary wavebands can be filtered flexibly and configured with any bandwidth steering to the output port independently.

In experiment, the diffraction efficiency of a 1201.2 line/mm grating is up to 92% at the blazing angle of 68° for telecom application. According to Eq. (4), the tuning resolution R is determined when $f = 145$ mm and $a = 3.74$ μm. The smaller pixel size can dramatically improve the tuning resolution. Fig. 7(a) shows the corresponding theoretical and measured values R. Although it is observed the grating loss distinctly increases from 0.4 dB at 68° up to 0.8 dB at 67°, the longer dispersion strip at 67° provides a finer tuning resolution in the range of 6.5 pm–8.5 pm according to the fitting curve in Fig. 7(a). On the other hand, the minimum spectral bandwidth B_{min} in Eq. (5) is proportional to (f/D), where D is the beam size in y-axis on the cylindrical lens. The larger D can reduce the beam spot in y-axis on chip for reducing minimum spectral bandwidth. The minimum spot size L_{min} in y-axis on chip is theoretically estimated 35 μm based on Eq. (6). The red line is ideal minimum 3 dB-bandwidth in Fig. 7(b) if the best perfect cylindrical lens was used in this system. However, due to the lens aberration and beam quality, the measured spot L_{min} is actually 50 μm in y-axis, beyond the diffraction limit. So, the fitting curve B_{min} of
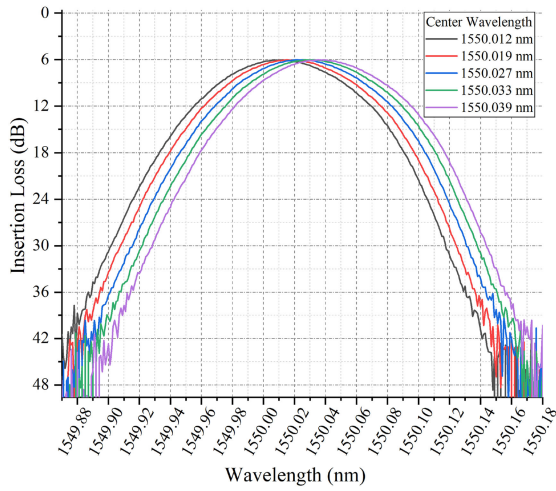
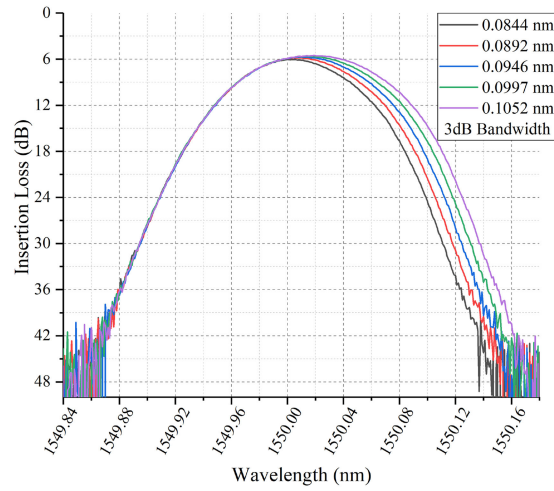Fig. 5. Wavelength tuning at the bandwidth of 10 GHz in filter.

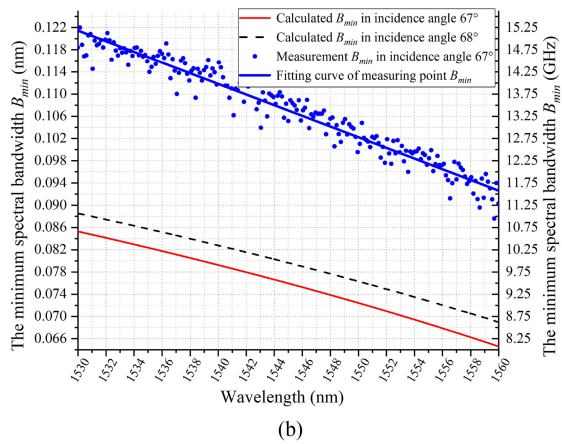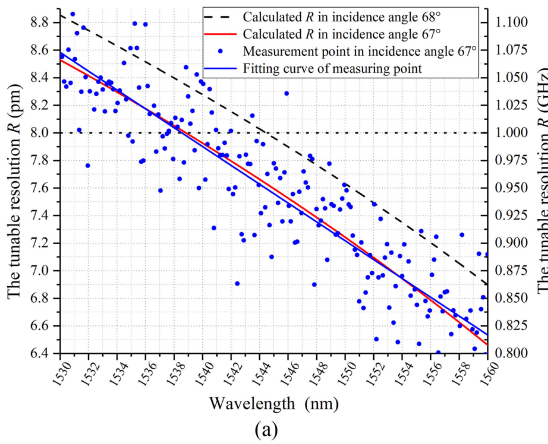Fig. 6. Flexible operation of channel 3 dB-bandwidth in filter.

Fig. 7. The tuning resolution of center wavelength (a) and the minimum spectral bandwidth (b) at different wavelength.

scatter plots in Fig. 7(b) indicates the minimum spectral bandwidth at different wavelength with no extra-loss.

The minimum and maximum bandwidth of this filter is 10 GHz and 3 THz across the entire C-band respectively. As shown in Fig. 8, the 3 dB-passband with center wavelength at 1550 nm ranges from 10 GHz to 100 GHz by a 10 GHz-step. The 10 GHz spectrum bandwidth introduces the additional 0.5 dB IL because Fig. 7(b) indicates the minimum bandwidth at 1550 nm is 12.6 GHz. The narrower bandwidth causes the larger IL. Although the narrower bandwidth can be obtained by reduce the number of pixels in hologram, the less number of pixels leads the more loss of light energy. For example, the bandwidth of 8.34 GHz is obtained with the expense of 3 dB extra loss in Fig. 8. Besides, the measured channel-crosstalk is less than −20 dB when the channel spacing is over 30 GHz. So it is believed that no channel-crosstalk for 50 GHz and 100 GHz spaced ITU-T channels for telecom application.

Furthermore, the optical filter is capable of attenuating the optical power. This functionality is advantageous as we can potentially balance power in a WSS by deflecting excess light away from the signal ports. The multi-casting phase holograms design is developed for LCoS chips, the diffraction light is split to a target output-port and other discarded ports. This discarded port is
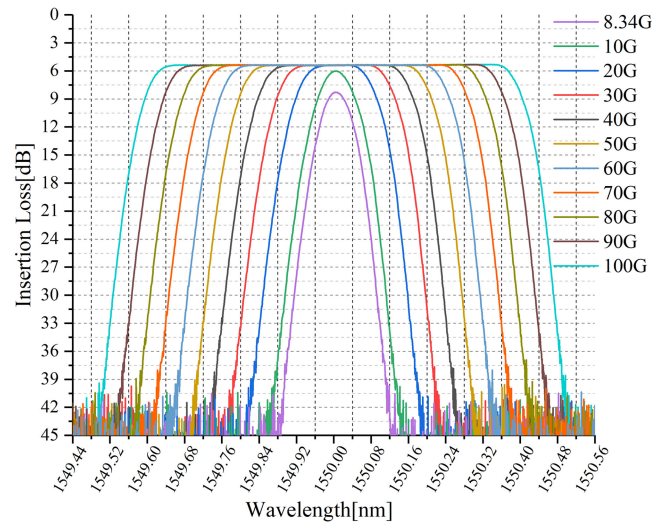
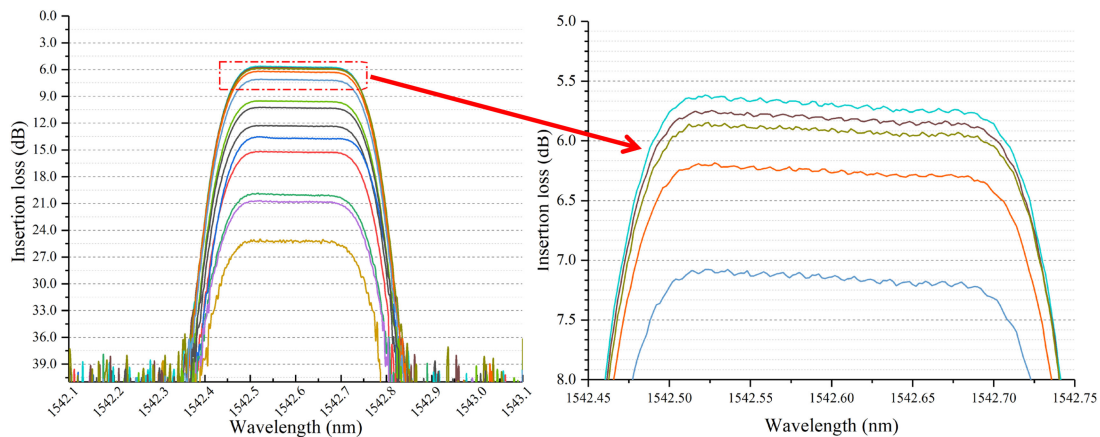Fig. 8. Flexible bandwidth from 8.34 GHz to 100 GHz.

Fig. 9. Optical power attenuation of optical filter.

selected to collect the excess energy to decrease the crosstalk in other output ports. If the time of pre-generated holograms is not considered, the switching time of LCoS is only determined by the image frame rate of 4k-LCoS. When resolution is set 3840 × 2160 pixels, the image frame rate is 30 Hz. But in reality, we must consider the time of generating holograms, so an efficient algorithm to generate the holograms is very important. In our work, a three-step algorithm is used to optimize the holograms: (1) the generation of the initial phase by Iterative Fourier Transform Algorithm (IFTA); (2) the generation of the weighted IFTA is to obtain the core hologram with continuous phase which cannot be directly applied in an LCoS; (3) the optimization of the core hologram by genetic algorithm for the final non-continuous phase hologram by configuring a suitable merit function. As shown in Fig. 9, the optical power attenuation is modulated from 0 dB to 30 dB with the resolution of 0.1 dB. Note that the ripples in Fig. 9 are caused by the gap between neighboring pixels in the LCoS.

4. Conclusions

We develop a high-resolution tunable filter by employing a 4k-LCoS, a 1201.2 line/mm transmission grating and a cemented cylindrical lens into the system. The proposed filter demonstrates the

flexibility and robust nature in the modulation of sub-GHz fine wavelength tuning, bandwidth and power attenuation. The total insertion loss is around 5.4 dB–6 dB over the entire C-band. The center wavelength of each channel can be tuned in the step of 7.5 $\pm$ 1 pm. The minimum and maximum 3 dB-bandwidth achieves 10 GHz and 3 THz respectively. Furthermore, by multi-casting hologram design techniques for an LCoS, the power attenuation is adjusted from 0 dB to 30 dB with the step of 0.1 dB. The performance is suitable for 50 GHz and 100 GHz ITU grid for telecom application.

Although it is convenient to apply the proposed filter into 1 $\times$ N WSS system, the performance needs to be improved further in three aspects: (1) the coupling efficiency of a fiber ribbon with a number of micro-lenses; (2) the diffraction efficiency of edge ports due to the fringing effect of electric field on an LCoS chip; (3) the crosstalk between multi-output ports still needs to be further reduced by optimizing the holograms.

References

[1] D. M. Marom *et al.*, "Survey of photonic switching architectures and technologies in support of spatially and spectrally flexible optical networking," *IEEE/OSA J. Opt. Commun. Netw.*, vol. 9, no. 1, pp. 1–26, Jan. 2017.

[2] J. Schröder, L. B. Du, J. Carpenter, B. J. Eggleton, and A. J. Lowery, "All-optical OFDM with cyclic prefix insertion using flexible wavelength selective switch optical processing," *J. Lightw. Technol.*, vol. 32, no. 4, pp. 752–759, Feb. 2014.

[3] J. Hoxha *et al.*, "Spectrally-efficient all-optical OFDM by WSS and AWG," *Opt. Exp.*, vol. 23, no. 9, pp. 10986–10996, 2015.

[4] L. B. Du, J. Schröder, M. M. Morshed, B. Eggleton, and A. J. Lowery, "Optical inverse Fourier transform generated 11.2-Tbit/s no-guard-interval all-optical OFDM transmission," in *Proc. Opt. Fiber Commun. Conf., Expo. Nat. Fiber Opt. Eng. Conf.*, 2013, Art. no. OW3B-5.

[5] M. Iwama *et al.*, "LCoS-based flexible grid 1 $\times$ 40 wavelength selective switch using planar lightwave circuit as spot size converter," in *Proc. IEEE Opt. Fiber Commun. Conf. Exhib.*, 2015, pp. 1–3.

[6] D. M. Marom, R. Rudnick, N. Goldstein, O. Golani, and D. Sinefeld, "Realization of sub-1 GHZ resolution photonic spectral processors for flexible optical networks," in *Proc. IEEE Eur. Conf. Opt. Commun.*, 2015, pp. 1–3.

[7] M. Iwama, M. Takahashi, Y. Uchida, and M. Kimura, "Low loss 1 $\times$ 93 wavelength selective switch using PLC-based spot size converter," in *Proc. Eur. Conf. Opt. Commun.*, 2015, pp. 1–3.

[8] T. Lu, N. Collings, B. Robertson, and D. Chu, "Design of a low-cost and compact 1 $\times$ 5 wavelength-selective switch for access networks," *Appl. Opt.*, vol. 54, no. 30, pp. 8844–8855, 2015.

[9] P. S. Khodashenas, J. M. Rivas-Moscoso, D. Klonidis, I. Tomkos, M. B. Shariati, and J. Comellas, "Impact of filter sharpness on the performance of elastic optical networks," in *Proc. IEEE Int. Conf. Commun.*, Jun. 2015, pp. 5192–5197.

[10] B. Robertson *et al.*, "Demonstration of multi-casting in a 1 $\times$ 9 LCoS wavelength selective switch," *J. Lightw. Technol.*, vol. 32, no. 3, pp. 402–410, Feb. 2014.

[11] D. Xie *et al.*, "LCoS-based wavelength-selective switch for future finer-grid elastic optical networks capable of all-optical wavelength conversion," *IEEE Photon. J.*, vol. 9, no. 2, Apr. 2017, Art. no. 7101212.

[12] Y. Sakurai *et al.*, "LCoS-based wavelength blocker array with channel-by-channel variable center wavelength and bandwidth," *IEEE Photon. Technol. Lett.*, vol. 23, no. 14, pp. 989–991, Jul. 2011.

[13] Z. Li, M. Zhang, D. Xie, D. Wang, Y. Cui, and Q. Yang, "LCoS-based programmable spectrum cutter with programmable and reconfigurable filtering shape for software defined optical network," in *Proc. Opto-Electron. Commun. Conf., Photon. Global Conf.*, 2017, pp. 1–4.

[14] M. Wang *et al.*, "LCoS SLM study and its application in wavelength selective switch," *Photonics*, vol. 4, no. 2, 2017, Art. no. 22.